 CMC, vol.14, no.3, pp.197-207, 2009

Measurements of the Curvature of Protrusions/Retrusions on Migrating Recrystallization Boundaries

Y.B. Zhang[1], A. Godfrey[2] and D. Juul Jensen[1]

Abstract: Two methods to quantify protrusions/retrusions and to estimate local boundary curvature from sample plane sections are proposed. The methods are used to evaluate the driving force due to curvature of the protrusions/retrusions for partially recrystallized pure nickel cold rolled to 96% reduction in thickness. The results reveal that the values calculated by both these methods are reasonable when compared with the stored energy measured by differential scanning calorimetry. The relationship between protrusions and the average stored energy density in the deformed matrix is also investigated for partially recrystallized pure aluminum cold rolled to 50%. The results show that the local deformed microstructure as well as local heterogeneities have to be analyzed in order to understand the formation of the protrusions.

Keywords: Recrystallization, protrusion and retrusion, electron backscattering patterns (EBSP), boundary curvature, stored energy.

1 Introduction

When a deformed metal is recrystallized, new essentially perfect nuclei develop and grow at the expense of the deformed matrix. Recrystallization is complete when the deformed matrix is fully replaced by a recrystallized grain structure. The driving force for the recrystallization is the energy stored in the deformed matrix [Haessner (2004)]. Classic recrystallization models generally assume nucleation at a random distribution of sites in the deformed microstructure and that all these nuclei grow with the same and with a constant (time independent) growth rate [e.g. Avrami (1939)]. However, this is not what typically occurs during recrystallization. In reality both the nucleation and the growth are highly heterogeneous [e.g.

[1] Danish-Chinese Center for Nanometals, Materials Research Division, RisøNational Laboratory for Sustainable Energy, Technical University of Denmark, DK-4000 Roskilde Denmark

[2] Laboratory of Advanced Materials, Dept. Material Science and Engineering, Tsinghua University, Beijing 100084, P.R. China

Vandermeer (2000); Storm and Juul Jensen (2009); Lauridsen, Poulsen, Nielsen and Juul Jensen (2003)]. Considering that lots of recent works on characterization of deformation microstructures have shown that these structures in most metals are highly heterogeneous [e.g. Hansen (2001)] and depend on the crystallographic orientations of the deformed grains [e.g. Huang and Winther (2007)], it is not so surprising that the recrystallization is non-homogeneous. However, mainly because of experimental limitations, not so much focus has been devoted yet to the effects of these inhomogeneities on recrystallization.

In-situ 3 dimensional x-ray diffraction (3DXRD) characterization of recrystallization of deformed single crystals [Schmidt, Nielsen, Gundlach, Margulies, Huang and Juul Jensen (2004)] has revealed that the growth during recrystallization, even in weakly deformed single crystals, is very inhomogeneous: the growth rates are different in different sample directions (e.g. along the rolling direction, RD and the normal direction, ND) [Juul Jensen and Schmidt (2009)], the migration of individual boundary segments occurs in a jerky stop-go type fashion, and locally fairly large protrusions (and retrusions) form on many boundaries. Concerning the stop-go type motion, ex-situ electron backscattering pattern (EBSP) investigations have later shown that the classic migration equation:

$$v = M \cdot F \tag{1}$$

where v is the growth rate, M the mobility and F the driving force, does not explain the local stop-go events [Zhang, Godfrey, Liu, Liu and Juul Jensen (2009)].

Concerning the protrusions, these are clearly visible also in many published micrographs of partly recrystallized metals, but not much attention was given to these local "anomalies" until the publication of the in-situ 3DXRD results. Some examples of protrusions are reproduced in Fig. 1. Also, following the 3DXRD measurements, several modeling schemes have been suggested which predict various types of protrusions [Martorano, Fortes and Padilha (2006); Godiksen, Trautt, Upmanyu, Schiotz, Juul Jensen and Schmidt (2007); Godiksen, Schmidt and Juul Jensen (2008); Sreekala and Haataju (2007)]. However, none of these models are yet at a level where they can reproduce and predict typical observations of protrusions.

The aim of the present work is to suggest methods to quantify experimental observations of protrusions/retrusions, to estimate the local boundary curvature of these, and to relate the results to the local deformation microstructure observed in front of a migrating recrystallization boundary. As examples partially recrystallized 50% cold rolled pure (99.996%) aluminum and 96% cold rolled pure (99.996%) nickel are used here.

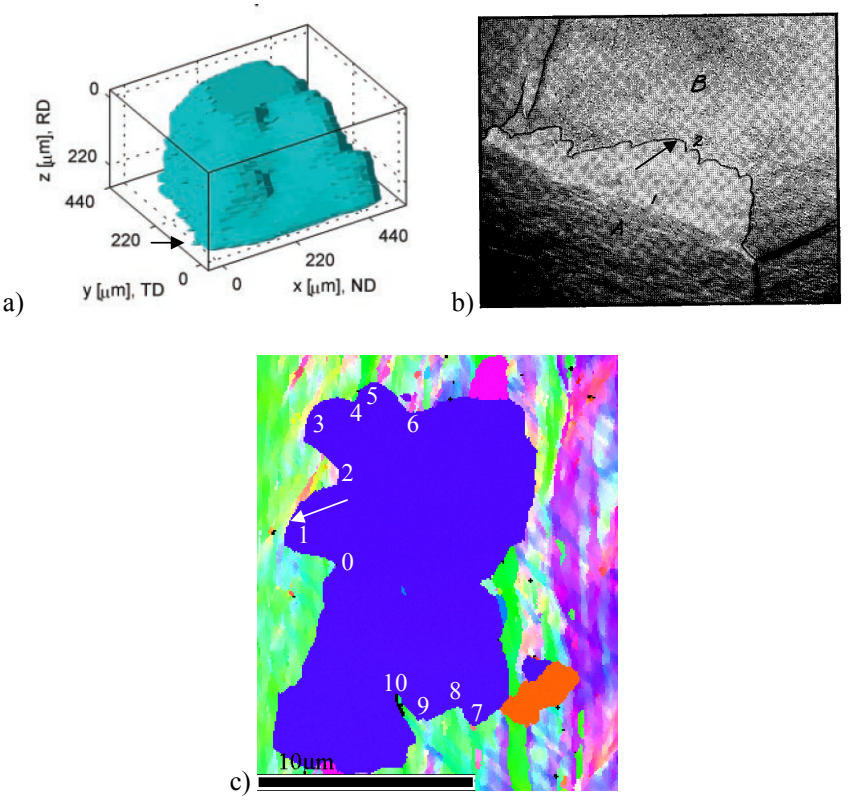

Figure 1: Some examples of micrographs showing protrusions on recrystallizing grains growing into deformed microstructures. Arrows are used to mark some of the protrusions. Protrusions are segments of the recrystallization boundary which have moved far further ahead than neighboring segments into the deformed matrix and appear as "peninsulas". In contrast retrusions, segments left behind, are also seen as "fjords" into the recrystallizing grain. a) 3DXRD snap shot of a recrystallizing grain in a 40% cold rolled aluminum alloy (AA1050) single crystal [Schmidt, Nielsen, Gundlach, Margulies, Huang and Juul Jensen (2004)]; b) strain induced boundary migration in high purity aluminum. Clear protrusions are seen when the boundary has moved from 1 to 2 [Beck, Sperry and Hu (1950)], and c) EBSP map of partially recrystallized 96% cold rolled pure (99.996%) nickel.

2 Quantifications of protrusions/retrusions

When a protrusion/retrusion is formed, it will increase the length of the recrystallizing boundary (which typically is a high-angle boundary), i.e. increase the

boundary energy. On the local scale, the boundary energy may thus also be important for evaluating the migration (and formation) of the protrusion and Eq. 1 can be written as:

$$v = M \cdot (F_D - F_\sigma) \tag{2}$$

where F_D and F_σ are the driving force contributions from the stored energy of the deformed structure and boundary curvature, respectively. This relationship implies that if a protrusion is formed, the local excess stored energy should be larger than the local boundary curvature at every boundary segments along the protrusion/retrusion (i.e. $F_D > F_\sigma$). The driving force induced by boundary curvature can be calculated using Eq. 3 [Humphreys and Hatherly (2004)]:

$$F_\sigma = \frac{2\sigma}{r} \tag{3}$$

where σ is the grain boundary energy, and r is the radius of the curvature of the boundary.

Two different methods to estimate the local radius of the boundary curvature of the protrusions/retrusions as observed in a sample plane are given in the following.

2.1 Method 1

Protrusions and retrusions often appear in an alternating fashion along a recrystallizing boundary, and the directions of radius of curvatures will consequently vary. Therefore, a simple sinusoidal shape is introduced to describe a protrusion and the neighbouring retrusion (a half shape is shown in Fig. 2a). This can be expressed by the equation:

$$y = A_0 + \Delta A \sin(\frac{2\pi}{\lambda}x - \frac{\pi}{2}) \tag{4}$$

where ΔA and λ are the amplitude and wavelength of the protrusion, and A_0 is a constant. The radius of the curvature can then be calculated by the well-known relation [Kreyszig (1991)]:

$$r = \frac{(1+\dot{y}^2)^{3/2}}{\ddot{y}} \tag{5}$$

It is obvious that the minimum radius of the curvature of the protrusion will be at $x = \lambda/2$ and $r_{\min} = \frac{-\lambda^2}{4\Delta A\pi^2}$. By inserting the minimum radius of curvature into Eq. 3 the maximum curvature driving force, $F_{\sigma max}$, within one protrusion is calculated:

$$F_{\sigma\max} = \frac{2\sigma}{r_{\min}} = \frac{-8\pi^2\sigma\Delta A}{\lambda^2} \tag{6}$$

It can be seen that the maximum driving force from the boundary curvature depends on the wavelength (λ) and the amplitude (ΔA) of the protrusion. In real microstructures the values for λ and ΔA of protrusions can be measured from EBSD maps as the distance between the top points of two neighboring retrusions and the half distance from the furthermost point of the protrusion between them to the line defining λ (as shown in Fig. 2b). The maximum driving force from curvature along the protrusion, which also reflects the required maximum excess stored energy in front of protrusion, can then be estimated using Eq. 6. Similarly, the maximum curvature driving force along the retrusion can also be estimated.

This sinusoidal shape method is easy to use, but it is clear that this is a coarse idealization as the shapes and the frequency of the protrusions/retrusions in general are not that symmetric. Therefore a second method is also derived to calculate $F_{\sigma max}$.

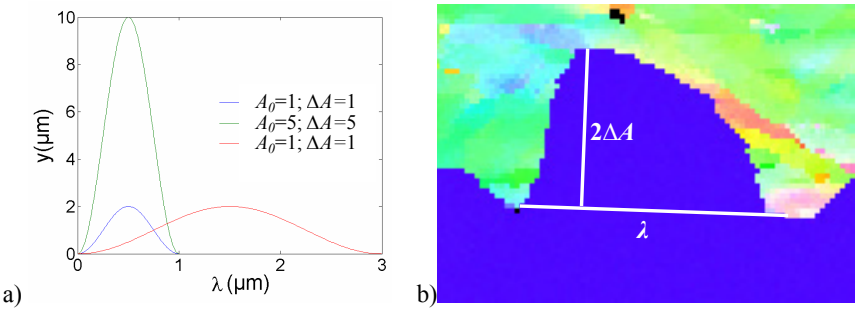

Figure 2: a) Illustration of an idealized sinusoidal shape of protrusions for different values of λ and ΔA, and b) example of measurement of λ and ΔA from an EBSD map.

2.2 Method 2

The local radii of the curvature along the migrating boundary can also be calculated directly by fitting using algebraic equations. For every pixel on the recrystallizing boundaries as observed in an EBSP map, a sub segment along the boundary containing 11 pixels, i.e. the actual pixel and 5 pixels on each side, can be extracted as shown in Fig. 3. The central pixel (x_i, y_i) is used as the coordinate of the central point of the protrusions. A local reference system (x',y') is fixed at the central pixel with x' parallel to the direction determined by the two neighboring pixels on each

side. The boundaries can then be fitted by using a polynomial equation:

$$y' = a_n x^n + a_{n-1} x^{n-1} + \cdots + a_1 x + a_0 \tag{7}$$

where n is the order of the polynomial and a_n is fitted to minimize the squared error between y' and the y'_i. In this work protrusions/retrusions have been fitted using n=5. The radius of curvature at each pixel can then be calculated using Eq. 5. The accuracy of this method depends on the step size of the EBSD measurements: a smaller step size will give a more accurate determination of the local boundary curvature.

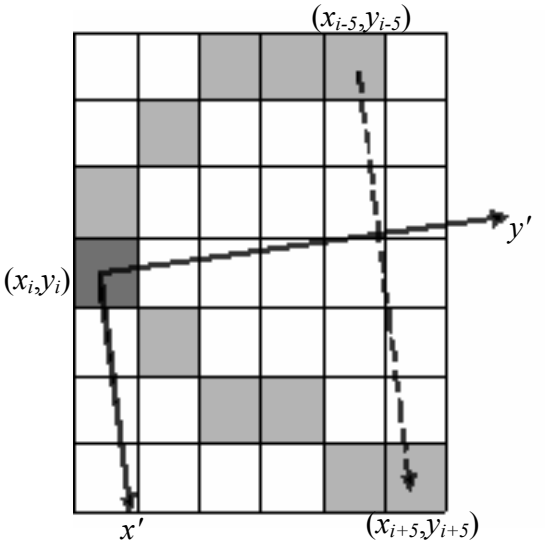

Figure 3: Illustration of method 2 showing pixels on a protrusion (grey pixels) and the local (x', y') coordinate system. The central pixel (x_i, y_i) is shown in dark grey.

2.3 Results of curvature calculation

The boundary curvature of the protrusions and retrusions numbered in Fig. 1c are estimated using these two methods. The maximum driving force corresponding to protrusions and retrusions are listed in Table. 1. In these calculations the grain boundary energy for nickel, σ = 0.866J/m^2 [Murr (1975)], is used. The two methods give $F_{\sigma max}$ values of the same sign for each individual protrusion but with very different values, which indicates the problems associated with the methods. The calculated values are in the range +17 to -65MJ/m^3. This seems fairly reasonable

as the overall average stored energy measured by differential scanning calorimetry (DSC) is about 13.6MJ/m^3 [Knudsen, Cao, Godfrey, Liu and Hansen (2008)]. It is, however, clear that DSC cannot be used to describe the protrusions as it does not capture the local deformed microstructure in which the boundary moves and the protrusions form. Also it should be noted that the calculated boundary curvature, and thus the $F_{\sigma max}$ values only represent a 2D section of the truly 3D shaped protrusions/retrusions.

Table 1: Maximum driving force due to boundary curvature estimated using the two different methods. The protrusions and retrusions are marked in Fig. 1c. A positive value of the driving force means that the boundary curvature is directed towards to the recrystallizing grain.

Num.	$2\Delta A(\mu$m)	$\lambda(\mu$m)	Method 1 $F_{\sigma maxx}$(MJ/m^3)	Method 2 $F_{\sigma max2}$(MJ/m^3)
0	0.94	2.45	-5.35	-31.6
1	2.44	4.03	5.14	8.1
2	1.93	4.6	-3.12	-9.5
3	1.98	3.56	5.34	16.8
4	0.55	2.36	-3.38	-14.4
5	1.12	2.75	5.06	10.7
6	1.15	4.32	-2.11	-9.5
7	0.84	1.92	7.79	10.4
8	0.84	2.45	-4.78	-11.3
9	0.97	2.83	4.14	10.5
10	1.08	0.75	-64.64	-46.0

3 Effect of the local deformed microstructure

The formation of protrusions and retrusions may be correlated to the heterogeneity of the stored energy in the deformed microstructure. Fig. 4 shows recrystallizing grains which grow into deformed microstructures of different orientations. The 3 grains each form protrusions of different morphology. In Fig. 4a very small protrusions have formed whereas in Fig. 4c very large protrusions are seen. Here protrusions on 2 levels are actually seen: large protrusions with relatively weak curvatures, and small ripple protrusions on top of these. The values of $2\Delta A/\lambda^2$ for all protrusions along one of the recrystallizing boundaries were estimated using method 1, and the average value of $2\Delta A/\lambda^2$ was calculated for each of the 3 examples in Fig. 4 together with data for 2 other grains. The stored energy den-

sity within the deformed matrix was also calculated using the method developed by Godfrey et al [Godfrey, Cao, Hansen and Liu (2005)]. Intuitively one would expect that large protrusions (i.e. large value of $2\Delta A/\lambda^2$) should correlate to large stored energy densities. The results for the 5 characterized grains are shown in Fig. 5. The figure, however, shows that the relation between the 2 parameters is not a simple linear relationship. A further understanding of this requires further experimental characterizations and quantifications.

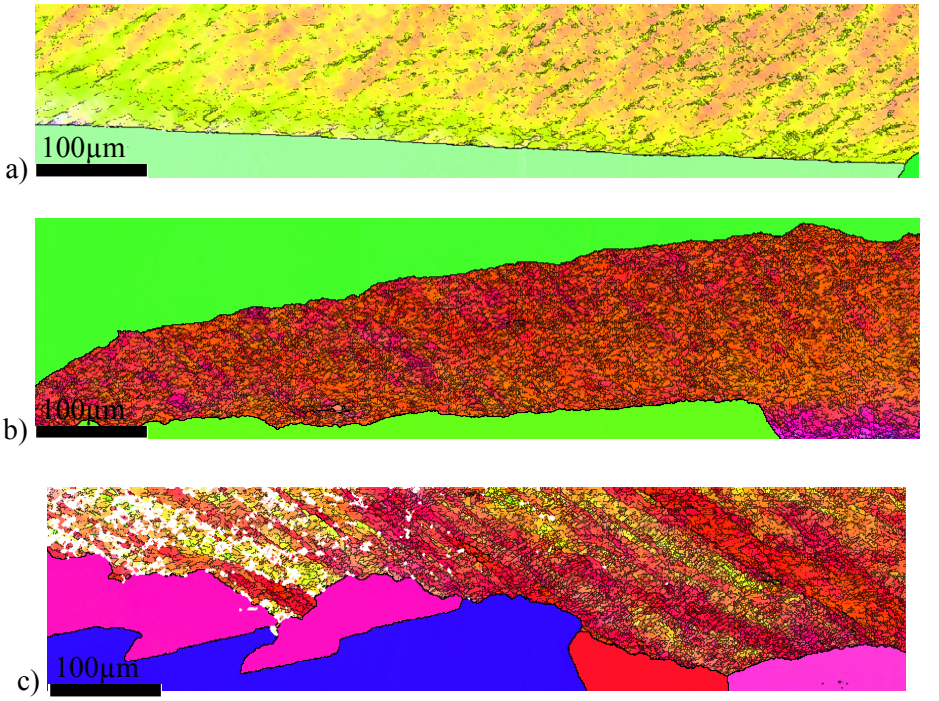

Figure 4: Examples EBSP maps showing the interface between recrystallizing grains and the deformed matrix of different orientations in pure Al cold rolled to 50% reduction.

Important elements of such further investigations would be to include the third dimension, to get better statistical data so that, for example, one large protrusion does not affect the average value (which it can in the analysis presented in Fig. 5), and to make direct small scale local correlations between individual protrusions and the local deformed microstructure (rather an average over a large boundary as is done in Fig. 5). Also the boundary character (including misorientation and

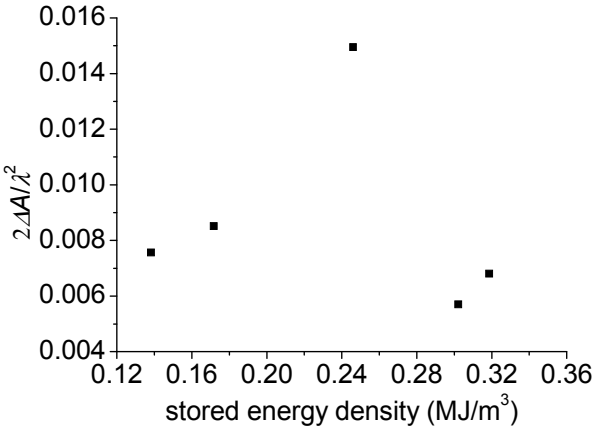

Figure 5: Average value of $2\Delta A/\lambda^2$ plotted vs. stored energy density for different deformed and recrystallizing grains.

boundary plane) should be considered in the analysis as the mobility may depend on this.

4 Conclusions and outlook

The formation of protrusions on boundaries between recrystallizing grains and deformed matrix is a common phenomenon and seems to be important for the migration of the recrystallization boundary. Because protrusions as well as retrusions lead to an increase in the boundary length as compared to a straight boundary, the boundary curvature and the additional local driving force have to be considered. Two methods to calculate the driving force due to curvature of the protrusions are presented, which give somewhat different values but both are in overall agreement with the average stored energy density of the entire deformed structure as measured by DSC. However, it is suggested that the the local deformed microstructure as well as local heterogeneities should be analyzed in 3D in order to understand the formation of the protrusions. Furthermore, it would be of interest to do in-situ investigations during annealing following the formation of protrusions in a well characterized deformed matrix, as well as to perform a statistical correlation analysis of the protrusions as a function of inhomogeneities in the deformed microstructures.

Acknowledgement: The authors gratefully acknowledge support from the Danish National Research Foundation and the National Natural Science Foundation of

China (Grant No. 50911130230) for the Danish-Chinese Center for Nanometals, within which this work was performed.

References

Avrami, M. (1939): Kinetics of phase change I – General theory. *J. Chem. Phys.*, vol. 7, pp. 1103-1112.

Beck, P.A.; Sperry, P.R.; Hu, H. (1950): The orientation dependence of the rate of grain boundary migration. *J. Appl. Phys.*, vol. 21, pp. 420-425.

Godfrey, A.; Cao, W.Q.; Hansen, N.; Liu, Q. (2005): Stored Energy, Microstructure and Flow Stress of Deformed Metals. *Metall. Mater. Trans.*, vol. 36A, pp. 2371-2378.

Godiksen, R.B.; Trautt, Z.T.; Upmanyu, M.; Schiøtz, J.; Juul Jensen, D.; Schmidt, S. (2007): Simulations of boundary migration during recrystallization using molecular dynamics. *Acta Mater.*, vol. 55, pp. 6383-6391.

Godiksen, R.B.; Schmidt, S.; Juul Jensen, D. (2008): Molecular dynamics simulations of grain boundary migration during recrystallization employing tilt and twist dislocation boundaries to provide the driving pressure. *Modeling Simul. Mater. Sci. Eng.*, vol. 16, pp. 065002.

Hansen, N. (2001): New discoveries in deformed metals. *Metall. Mater. Trans.*, vol. 32A, pp. 2917-2935.

Haessner, F. (1978): *Recrystallization of metallic materials.* Dr. Riederer Verlag GmbH Stuttgart.

Huang, X.; Winther, G. (2007): Dislocation structures. Part I. Grain orientation dependence. *Phil. Mag.*, vol. 87, pp. 5189-5214.

Juul Jensen, D.; Schmidt, S. (2009): Time Evolution in 3D Metal Microstructures-Recrystallization. *Mater. Trans.*, vol. 50, pp. 1655-1659.

Knudsen, T.; Cao, W.Q.; Godfrey, A.; Liu, Q.; Hansen, N. (2008): Stored energy in nickel cold rolled to large strains, measured by calorimetry and evaluated from the microstructure. *Metall. Mater. Trans.*, vol. 39A, pp. 430-440.

Kreyszig, E. (1991): *Differential geometry.* Dover Publications.

Lauridsen, E.M.; Poulsen, H.F.; Nielsen, S.F.; Juul Jensen, D. (2003): Recrystallization kinetics of individual bulk grains in 90% cold-rolled aluminium. *Acta Mater.*, vol. 51,pp. 4423-4435.

Martorano, M.A.; Fortes, M.A.; Padilha, A.F. (2006): The growth of protrusions at the boundary of a recrystallized grain. *Acta Mater.*, vol. 54, pp.2769-2776.

Murr, L.E. (1975): *Interfacial Phenomena in Metals and Alloys.* Addison-Wesley,

Reading, pp. 131.

Schmidt, S.; Nielsen, S.F.; Gundlach, C.; Margulies, L.; Huang X.; Juul Jensen, D. (2004): Watching the growth of bulk grains during recrystallization of deformed metals. *Science*, vol.305, pp. 229-232.

Sreekala, S.; Haataja, M. (2007): Recrystallization kinetics: A coupled coarse-grained dislocation density and phase-field approach. *Phys. Rev. B*, vol. 76, pp. 094109.

Storm, S.; Juul Jensen, D. (2009): Effects of clustered nucleation on recrystallization. *Scripta Mater.* Vol. 60, pp. 477-480.

Vandermeer, R.A. (2000): Kinetic aspects of nucleation and growth in recrystallization. Proceedings of the 21st Risø International Symposium. Vol. 21, pp. 179-200.

Zhang, Y.B.; Godfrey, A.; Liu, Q.; Liu, W.; Juul Jensen, D. (2009): Analysis of the growth of individual grains during recrystallization in pure nickel. *Acta Mater.*, vol. 57, pp. 2632-2639.